Clustered Ribbed-Nanoneedle Structured Copper Surfaces with High-Efficiency Dropwise Condensation Heat Transfer Performance

Jie Zhu,[†] Yuting Luo,[†] Jian Tian, Juan Li, and Xuefeng Gao*

Advanced Thermal Nanomaterials and Devices Research Group, Nanobionic Division, Suzhou Institute of Nano-Tech and Nano-Bionics, Chinese Academy of Sciences, Suzhou 215123, P. R. China

S *Supporting Information*

ABSTRACT: We report that the dropwise condensation heat transfer (DCHT) effectiveness of copper surfaces can be dramatically enhanced by in situ grown clustered ribbed-nanoneedles. Combined experiments and theoretical analyses reveal that, due to the microscopically rugged and low-adhesive nature of building blocks, the nanosamples can not only realize high-density nucleation but constrain growing condensates into suspended microdrops via the self-transport and/or self-expansion mode for subsequently self-propelled jumping, powered by coalescence-released excess surface energy. Consequently, our nanosample exhibits over 125% enhancement in DCHT coefficient. This work helps develop advanced heat-transfer materials and devices for efficient thermal management and energy utilization.

KEYWORDS: *superhydrophobic, clustered ribbed-nanoneedles, condensate microdrop self-propelling, high-density nucleation, enhanced heat transfer*
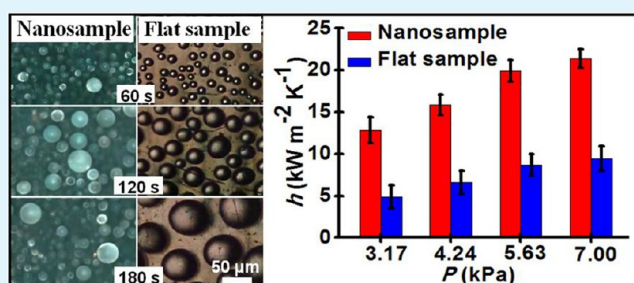
Vapor−liquid phase-change heat transfer is a type of widely used energy transport way, which has a pivotal role in modernized human life and industrial processes from the viewpoint of either thermal management or energy utilization.[1−7] Since the 1930s, scientists have realized that compared with filmwise condensation, dropwise condensation is a type of more efficient heat transfer mode because discrete condensate drops have far lower thermal resistance than continuous liquid films and can release far more bare surface sites for performing more cycles of nucleation, growth and departure.[8−11] However, condensate drops on the usual flat metal surfaces still have relatively higher thermal resistance, slower renewal frequency and lower density because they cannot shed off under gravity until growing into the millimeter scale. Recent studies have indicated that the dropwise condensation heat transfer (DCHT) coefficient can be enhanced by a type of innovative condensate microdrop self-propelling (CMDSP) surfaces,[4−7] which can realize the efficient self-departure of small-scale condensate microdrops via coalescence-released excess surface energy without requiring external forces such as gravity and steam shear force. For example, Miljkovic et al. first reported that the DCHT coefficient can be enhanced ∼30% by the in situ growth of CMDSP blade-like CuO nanostructures on copper surface.[6] Recently, Hou et al. have demonstrated that the DCHT coefficient can be enhanced up to ∼63% by the smart design of a bionic CMDSP silicon nanoneedle structure inserted with patterned micropillars, which tops are coated by hydrophilic silica to increase the density and growth rate of condensates.[7] However, such hybrid structure cannot be in situ

integrated into metal surfaces, restricted by top-down nano-fabrication technologies. Clearly, it is still very challenging to achieve metal-based high-efficiency DCHT surfaces up to now. Therefore, it is significant to explore metal-based CMDSP nanostructures with higher DCHT effectiveness and their structure−property relationships.

Here, we report that the DCHT effectiveness of copper surfaces can be dramatically enhanced by in situ growth of clustered ribbed-nanoneedles. Combined experiments and theoretical analyses reveal that, due to the microscopically rugged and low-adhesive nature of building blocks, the nanosamples can not only realize high-density nucleation but constrain growing condensates into suspended microdrops via the self-transport and/or self-expansion mode for subsequently self-propelled jumping, powered by coalescence-released excess surface energy. As a result, the nanosample exhibits over ∼125% enhancement in the DCHT coefficient, as compared to that of the flat copper sample with identical surface chemistry. These findings help develop advanced heat and mass transfer nanomaterials and devices.

Figure 1a-c show typical scanning electronic microscopic (SEM) images of the as-prepared clustered copper hydroxide ribbed-nanoneedle films (Synthesis details see Experimental Section in Supporting Information). These in situ grown nanoneedles on copper substrates present not only microscopic
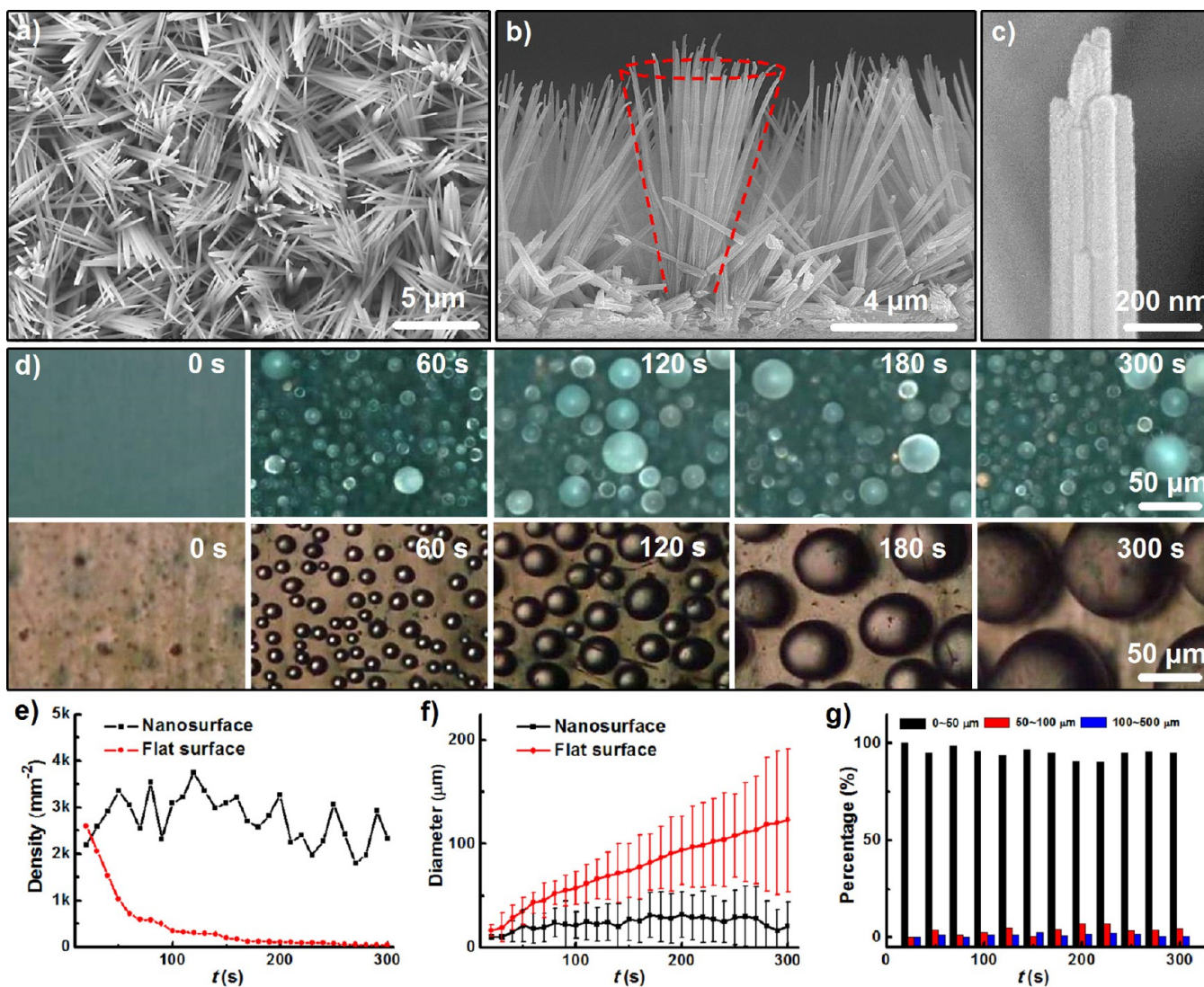
Figure 1. (a, b) Typical SEM top-view and side-view of the clustered copper hydroxide ribbed-nanoneedles, which are in situ grown on copper substrates followed by hydrophobicization. (c) Magnified side-view of a single nanoneedle, showing the detail of its tip and ribbed sidewall. (d) Time-lapse optical top-view images of vertical nanostructured (top) and flat (bottom) samples at the condensation condition of $T_s \sim 1$ °C, $T_{air} \sim 22$ °C, and RH $\sim 80\%$. (e, f) Density and diameter of condensate drops on the nanostructured (black) and flat (red) surface varied with condensation time. (g) Statistic drop number percentage of condensed microdrops with diameters of <50 μm (black), 50−100 μm (red), and 100−500 μm (blue) on the nanostructured surface. Clearly, such nanostructured film owns the remarkable high-density self-renewal ability of small-scale condensate microdrops.

3D rugged feature but radial nanoneedle clusters with needle-to-needle interspaces tapering from the top down. The average diameter of nanoneedles is tapering from ∼800 nm at the base down to ∼150 nm at the tip while their average length is ∼8 μm. Remarkably, the lateral surface of each nanoneedle is sculptured with hierarchical nanogrooves along the longitudinal direction. After fluorosilane modification, the nanostructured surface could realize the high-density self-renewal of small-scale condensate microdrops in comparison with the contrast flat surface with identical surface chemistry. Figure 1d shows the distinct condensation behaviors on the surface of the vertically placed nanostructured (top row) and flat (bottom row) samples at the condition of substrate temperature (T_{sub}) ∼1 °C, ambient temperature (T_{air}) ∼22 °C, and relative humidity (RH) ∼80%. Evidently, the nanostructured surface always owns far higher density of condensate microdrops with fluctuated sizes, whereas the size of condensate drops on the flat surface

can rapidly increase, accompanied by the decrease of the drop number density (Figure 1d and Figure S1 in the Supporting Information).

To more intuitively compare the difference of the nanostructured surface and flat surface in the nucleation density and self-departure abilities of condensate microdrops, we first conduct statistical analysis into the number density (Figure 1e) and average diameter (Figure 1f) of residence drops, respectively. With the time extending, the number density of drops on the nanostructured surface always present a fluctuation (with the average density of ∼2755 mm^{-2}), in sharp contrast to their rapid decrease trend on the flat surface. Besides, the average diameters of all drops on the nanostructured surface always maintain around 23 μm during the whole condensation periods. In contrast, the drops on the flat surface can rapidly grow up via mutual coalescence, which sizes can reach 100 μm only within ∼200 s. To further highlight the
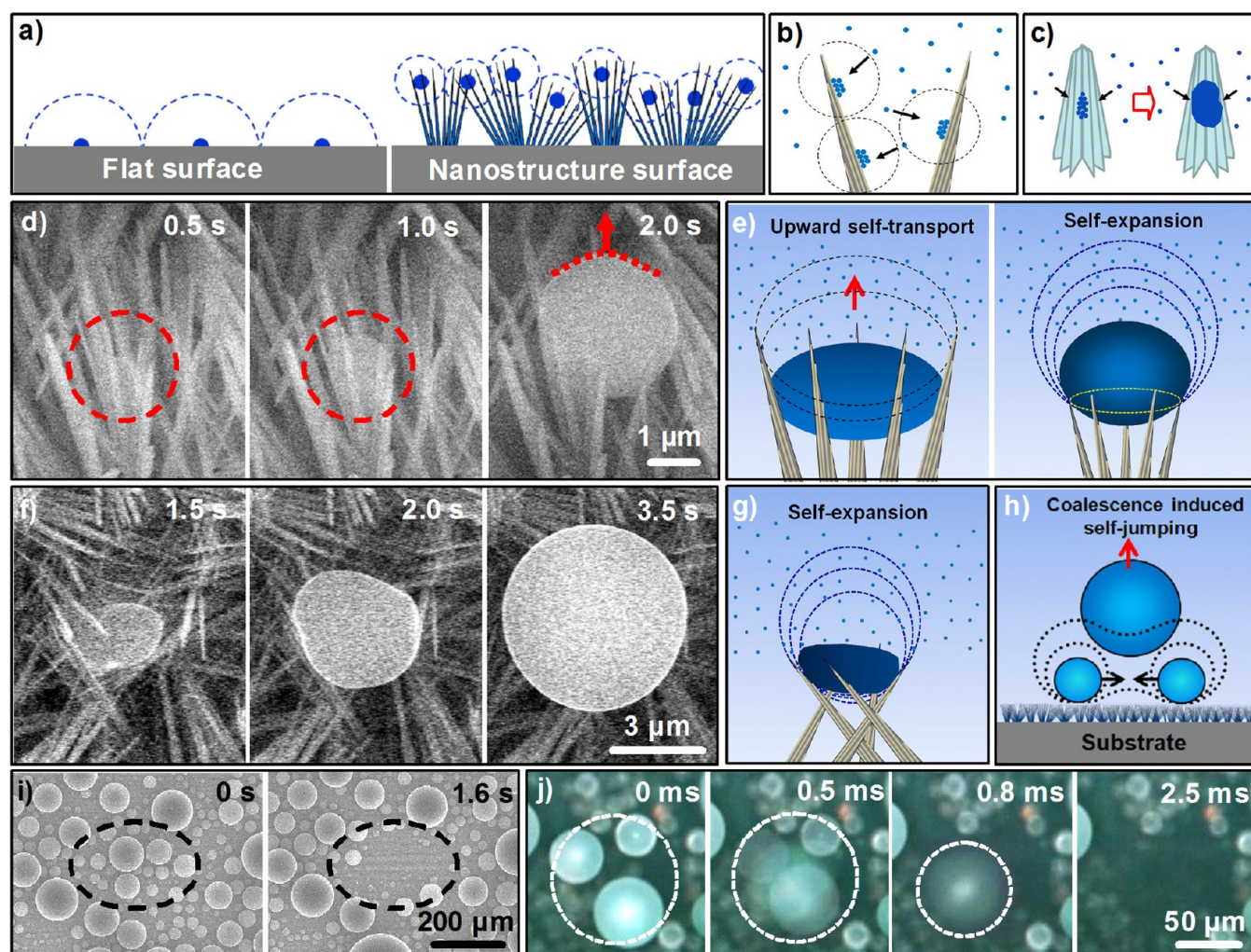
Figure 2. (a−c) Schematics of high-density nucleation based on three nanostructure effects: (a) the higher specific surface area due to 3D microscopic roughness; (b) increasing trapping efficiency of collided water clusters due to microscale inverse-conical pits within the nanoneedle "forest"; and (c) decreasing the energy barrier of heterogeneous nucleation due to the ribbed nanotexture of the nanoneedle sidewall. (d−j) The self-transport mechanism of condensate on the clustered ribbed-nanoneedle films: (d, e) ESEM top-views and schematic showing the typical self-transport and self-expansion modes of condensate forming inside the clustered ribbed-nanoneedles; (f, g) ESEM top-views and schematic showing the typical self-expansion mode of condensate forming atop the clustered ribbed-nanoneedles; (h−j) Schematic, ESEM images and optical top-views showing the coalescence-induced self-jumping of condensate microdrops.

nanostructure-induced microdrop self-departure ability at smaller scale, we analyze the drop number percentage of residence microdrops with diameters (d) of <50 μm, 50−100 μm, and 100−500 μm, as shown in Figure 1g. Clearly, condensate drops with d < 50 μm occupy over 90% of the total number despite slight fluctuation with time, whereas larger sizes of drops occupy only <10%. Compared with the flat surfaces, such nanostructures can not only induce higher density of condensed microdrops but reduce their residence sizes by at least 1 order of magnitude.

It is easily understood that these condensation events occurred on the nanostructured surface are a complex dynamic process of spanning multiple spatial dimensions with the time extending, which includes initial adsorption of vapor clusters, nucleation, direct vapor condensation growth, coalescence-governed growth and self-departure.[1,2,12] However, the direct imaging of the former three stages is still an unrealizable task, restricted by microscopic imaging technologies. Even so, we can qualitatively interpret the mechanisms why the density of condensate microdrops on the nanostructured surface is so

high. On the basis of reasonable analysis, we suppose that the increased density of residence microdrops mainly may be ascribed to three nanostructure effects, in comparison with the contrast flat surface. First, as shown in Figure 2a, the microscopic 3D rugged nanostructure can provide far higher specific surface area for condensation nucleation.[13] Second, the nanoneedle "forests" with numerous microscale pits help increase the trapping efficiency of collided water clusters (Figure 2b). Third, the hierarchical nanotexture on the surface of the ribbed-nanoneedle sidewall may help decrease the energy barrier of heterogeneous nucleation,[1,12,13] increasing the nucleation efficiency (Figure 2c).

Another issue we concerned is why the nanostructure can realize the efficient self-departure of small-scale condensate microdrops and simultaneously avoid the penetration of moisture during the condensation process. To address the corresponding physical mechanisms, we have investigated into the details of condensate growth, microdrop coalescence and self-departure using the state-of-the-art microscopic imaging technologies. First, the growth behaviors of condensate heavily

depend on their locations at the microscale. We found that condensate, formed inside the inverse-conical nanoneedle cluster, can gradually grow larger and transport upward during a very short duration (~2.0 s), as shown in Figure 2d. We suppose that the upward self-transport of these tiny condensate microdrops during the condensation growth process may be mainly ascribed to the unbalanced Laplace pressure,[14−16] which originates from the asymmetric structure induced curvature difference between the top and bottom surfaces (left of Figure 2e). Note that the tapered nanoneedle structure can also help the upward movement of bottom liquid−solid−air contact lines, which lifting force increases linearly with the length of the restricted grown condensates along the normal direction,[17,18] whereas the hierarchical nanogrooves on the sidewalls of nanoneedles can reduce the solid−liquid interface adhesion.[19] On the other hand, irregular tiny condensates formed on the top-layer sites can rapidly grow and gradually expand into a suspended spherical microdrop (Figure S2 in the Supporting Information). Figure 2f, g show the corresponding top-view environmental scanning electronic microscopic (ESEM) images and schematic, respectively. Such self-expansion event also occurs during the later growth process of the self-transported microdrops, as shown in the right panel of Figure 2e. Subsequently, these suspended microdrops can realize the self-departure via their mutual coalescence (Figure 2h), as proofed by ESEM images (Figure 2i) and high-speed optical microscopic images (Figure 2j). Such self-departure results from the extremely low solid−liquid adhesion of the clustered ribbed-nanoneedle structure (Figure S3 in the Supporting Information),[19−22] where excess surface energy released from the coalescence of microdrops is sufficient to drive the self-departure of the merged microdrops.[21]

It should be pointed out that water molecules are prone to self-aggregate into water clusters (with sizes far larger than water molecules) above the subcooled substrate and absorb at the near-surface sites of lateral walls of nanoneedles to form numerous nanoscale condensate drops,[23] which can rapidly grow via preferential absorption of ambient moisture due to water affinity.[24] As a result, submicrometer-scale water bridges can easily form among the multiple hydrophobic ribbed-nanoneedles. Because of the extremely strong capillary pressure,[20] the menisci can effectively prevent the downward penetration of trace water with irregular shapes restricted by space geometry (Figure 2d−g). As the irregular condensate drops further grow, their upper surface gradually presents a spherical crown shape due to the inherent minimization need of the system's total surface energy, accompanied by the self-expanding (like blowing a balloon) of "top" condensate microdrops (Figure 2d) and the upward self-transport and self-expanding of "inner" condensate microdrops (Figure 2f). Accordingly, moisture cannot penetrate into the valley bottom of closely packed hydrophobic nanoneedles during the whole condensation process. On the other hand, the high-density nucleation is advantageous to the relatively uniform growth and accelerated coalescence of condensate microdrops at smaller scale due to the reduced distances among adjacent drops, finally resulting in the efficient self-departure of small-scale condensate microdrops. In fact, such remarkable small-scale condensate microdrop self-renewal ability can help release far more surface sites for performing more cycles of nucleation, growth and departure per unit area and per unit time, in sharp contrast to the gravity-driven dropwise condensation behaviors on the flat surface.
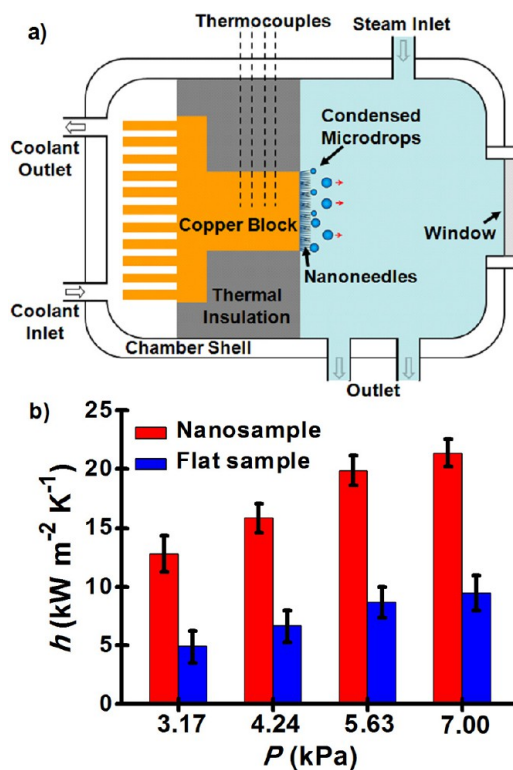

Figure 3. (a) Principle diagram for measuring the condensation heat transfer performance. (b) Dropwise condensation heat transfer coefficient (h) of the nanostructured (red) and flat (blue) surfaces under varied vapor pressure (P). The condensation heat transfer coefficient of copper surface can be dramatically enhanced by surface nanoengineering.

The effects of high-density condensation nucleation and small-scale microdrop self-departure can be used for enhancing the condensation heat transfer property. Figure 3a shows a measuring principle diagram. To ensure one-dimensional axial steady-state heat transfer, a fin-integrated cylindrical copper block (Figure S4a in the Supporting Information) is inserted into a Teflon insulator that divides a steel chamber into a condensation chamber (right) and a cooling chamber (left). Via regulating the pressure (P) of saturated vapor (with the corresponding temperature, T_v) and the temperature of coolant (with a fixed flow rate), we can measure the temperature gradient (∇T) within the copper block using equidistant thermocouples, which can be used for calculating the surface temperature (T_s). As a result, the DCHT coefficient (h) of the samples can be obtained by the equation $h = k \cdot \nabla T / \Delta T$, where k is the thermal conductivity of copper and ΔT is the degree of wall subcooling (i.e., the difference between T_v and T_s). Measurement Details see Experimental Section in Supporting Information. In general, it is highly desirable to achieve higher h values at lower ΔT. In view of common feature that the h values decrease with the increase of ΔT, we only present and compare the h values of the nanostructured and flat samples under varied P while fixing $\Delta T = 1.3 \pm 0.1$ K (Figure 3b), which is the minimum avaliable for accurately measuring the h values in this case. It was found that the h values of the nanosamples are apparently higher than that of the flat samples and can increase with the increase of saturated vapor pressure. However, their enhancement factor, defined as $(h_{nano} - h_{flat})/h_{flat}$, is slightly decreased from ~1.62 ($P = 3.17$ kPa), down to ~1.39 ($P = 4.24$ kPa), ~1.29 ($P = 5.63$ kPa), and ~1.25 ($P =

7.00 kPa), respectively. Clearly, the DCHT coefficient of copper surfaces can be enhanced over ~125% by the in situ growth of CMDSP clustered ribbed-nanoneedle films.

The slight decline in the heat-transfer enhancement factors of the nanosamples accompanied by the increase of vapor pressure can be ascribed to two reasons as follows. First, the wettability and surface adhesion of condensate drops are closely related to their temperature. It is easily understood that higher vapor temperature can induce stronger "wetting" ability of the condensate drops due to their reduced interface tension, which inevitably increase the solid−liquid interface adhesion.[25] As a result, condensate microdrops must grow up to a relatively larger size at higher vapor temperature until the surface energy released from their coalescence is sufficient to overcome the droplet−surface interface adhesion. The larger residence microdrops would result in relatively larger thermal resistance and more energy dissipation during the phase change energy transport. Second, the nucleation rate and density of condensate drops can be apparently promoted with the increase in vapor pressure. Accordingly, microscopic condensate drops can quickly merge with other adjacent condensates, which slow down their self-renewal frequency. In fact, the accelerated nucleation caused by the increase in vapor pressure helps enhance the mass and heat transfer, which, however, can be compromised by the increased interface adhesion.

It is well-known that the DCHT coefficient also depends on the thermal resistance of film layers. Recently, Miljkovic et al. have proposed on the basis of model analyses that, as the thickness of superhydrophobic nanostructured films is beyond 2 μm, their DCHT performance would be inferior to that of hydrophobic flat surfaces.[26] Surprisingly, our nanosamples possess apparently higher DCHT coefficients than that of the flat surface, despite the thickness of CMDSP films reaching ~8 μm (it is very difficult to fabricate thinner CMDSP films in this case). We believe that such higher DCHT effectiveness may be ascribed to the nanostructure-induced remarkable high-density self-renewal ability of small-scale condensate microdrops. It should also be pointed out that our nanosample exhibits apparent higher enhancement factors in the DCHT coefficient, as compared to the previous reported data,[6,7] and the absolute values of our measured DCHT coefficients are lower than those reported by Miljkovic et al.,[6] which may be ascribed to the higher content of noncondensable gas,[2,9] restricted by the vacuum ability of our used thermal measurement setup. Clearly, either the DCHT coefficients or enhancement factors of the as-prepared clustered ribbed-nanoneedle film may be further optimized in the near future.

In summary, we have demonstrated a smart strategy of utilizing clustered hydrophobic ribbed-nanoneedles, in situ grown on copper surfaces, to simultaneously realize the high-density nucleation and self-departure of small-scale condensate microdrops for substantially enhancing DCHT performance. The mechanisms of nanostructure-induced high-density nucleation and small-scale microdrop self-departure, involving the site-dependent restriction growth of condensate toward suspended microdrops, are rationalized based on detailed microscopic imaging combined with theoretical analyses. Our preliminary thermal characterization indicate that the DCHT coefficient of copper surface can be enhanced over 125% via the in situ grown ribbed-nanoneedles. In principle, any nanostructure may be an alternative only if it owns microscopic 3D roughness and low solid−liquid adhesion nature,[27] which helps

develop advanced DCHT nanomaterials and devices for most efficient thermal management and energy utilization. In addition, these findings help develop energy-saving frost-free nanotechnologies for such heat exchangers as air-conditioners and refrigerators.[28]

■ ASSOCIATED CONTENT

ⓢ Supporting Information

Experimental Section, distinct transport modes of condensate drops on the nanostructured and contrast flat sample surface (Figure S1), the ESEM top-views showing the droplet self-expansion growth mode (Figure S2), the solid−liquid low-adhesive properties of nanosamples (Figure S3) and the optical image of nanostructured copper specimen and the exemplified curve of heat flux and heat transfer coefficient versus the degree of subcooling (Figure S4). The Supporting Information is available free of charge on the ACS Publications website at DOI: 10.1021/acsami.5b02376.

■ AUTHOR INFORMATION

Corresponding Author
*E-mail: xfgao2007@sinano.ac.cn.

Author Contributions
†J.Z. and Y.L. contributed equally.

Notes
The authors declare no competing financial interest.

■ REFERENCES

(1) Carey, V. P. *Liquid-Vapor Phase-Change Phenomena*; Taylor and Francis: London, 2008.

(2) Miljkovic, N.; Wang, E. N. Condensation Heat Transfer on Superhydrophobic Surfaces. *MRS Bull.* **2013**, *38*, 397−406.

(3) Enright, R.; Miljkovic, N.; Alvarado, J. L.; Kim, K.; Rose, J. W. Dropwise Condensation on Micro- and Nanostructured Surfaces. *Nanoscale Microscale Thermophys. Eng.* **2014**, *18*, 223−250.

(4) Boreyko, J. B.; Zhao, Y.; Chen, C.-H. Planar Jumping-Drop Thermal Diodes. *Appl. Phys. Lett.* **2011**, *99*, 234105.

(5) Boreyko, J. B.; Chen, C.-H. Vapor Chambers with Jumping-Drop Liquid Return from Superhydrophobic Condensers. *Int. J. Heat Mass Transfer* **2013**, *61*, 409−418.

(6) Miljkovic, N.; Enright, R.; Nam, Y.; Lopez, K.; Dou, N.; Sack, J.; Wang, E. N. Jumping-Droplet-Enhanced Condensation on Scalable Superhydrophobic Nanostructured Surfaces. *Nano Lett.* **2013**, *13*, 179−187.

(7) Hou, Y.; Yu, M.; Chen, X.; Wang, Z.; Yao, S. Recurrent Filmwise and Dropwise Condensation on a Beetle Mimetic Surface. *ACS Nano* **2015**, *9*, 71−81.

(8) Schmidt, E.; Schurig, W.; Sellschopp, W. Versuche über die Kondesation von Wasserdampf in Film- und Tropfenform. *Forsch. Ingenieurwes.* **1930**, *1*, 53−63.

(9) Rose, J. W. Dropwise Condensation Theory and Experiment: A review. *Proc. Inst. Mech. Eng. Part A* **2002**, *216*, 115−128.

(10) Daniel, S.; Chaudhury, M. K.; Chen, J. C. Fast Drop Movements Resulting from the Phase Change on a Gradient Surface. *Science* **2001**, *291*, 633−636.

(11) Chen, J. C. Surface Contact-Its Significance for Multiphase Heat Transfer: Diverse Examples. *J. Heat Transfer* **2003**, *125*, 549−566.

(12) Sikarwar, B. S.; Khandekar, S.; Agrawal, S.; Kumar, S.; Muralidhar, K. Dropwise Condensation Studies on Multiple Scales. *Heat Transfer Eng.* **2012**, *33*, 301−341.

(13) Mu, C.; Pang, J.; Lu, Q.; Liu, T. Effects of Surface Topography of Material on Nucleation Site Density of Dropwise Condensation. *Chem. Eng. Sci.* **2008**, *63*, 874−880.

(14) Zheng, Y.; Han, D.; Zhai, J.; Jiang, L. In Situ Investigation on Dynamic Suspending of Microdroplet on Lotus Leaf and Gradient of Wettable Micro- and Nanostructure from Water Condensation. *Appl. Phys. Lett.* **2008**, *92*, 084106.

(15) Zheng, Y.; Bai, H.; Huang, Z.; Tian, X.; Nie, F.-Q.; Zhao, Y.; Zhai, J.; Jiang, L. Directional Water Collection on Wetted Spider Silk. *Nature* **2010**, *463*, 640−643.

(16) Ju, J.; Bai, H.; Zheng, Y.; Zhao, T.; Fang, R.; Jiang, L. A Multi-Structural and Multi-Functional Integrated Fog Collection System in Cactus. *Nat. Commun.* **2012**, *3*, 1247.

(17) D'Urso, B.; Simpson, J. T.; Kalyanaraman, M. Emergence of Superhydrophobic Behavior on Vertically Aligned Nanocone Arrays. *Appl. Phys. Lett.* **2007**, *90*, 044102.

(18) Liu, Y.; Moevius, L.; Xu, X.; Qian, T.; Yeomans, J. M.; Wang, Z. Pancake Bouncing on Superhydrophobic Surfaces. *Nat. Phys.* **2014**, *10*, 515−519.

(19) Yao, X.; Chen, Q.; Xu, L.; Li, Q.; Song, Y.; Gao, X.; Quéré, D.; Jiang, L. Bioinspired Ribbed Nanoneedles with Robust Super-hydrophobicity. *Adv. Funct. Mater.* **2010**, *20*, 656−662.

(20) Quéré, D. Non-Sticking Drops. *Rep. Prog. Phys.* **2005**, *68*, 2495−2532.

(21) Tian, J.; Zhu, J.; Guo, H.-Y.; Li, J.; Feng, X.-Q.; Gao, X. Efficient Self-Propelling of Small-Scale Condensed Microdrops by Closely Packed ZnO Nanoneedles. *J. Phys. Chem. Lett.* **2014**, *5*, 2084−2088.

(22) Lai, Y.; Gao, X.; Zhuang, H.; Huang, J.; Lin, C.; Jiang, L. Designing Superhydrophobic Porous Nanostructures with Tunable Water Adhesion. *Adv. Mater.* **2009**, *21*, 3799−3803.

(23) Song, T.; Lan, Z.; Ma, X.; Bai, T. Molecular Clustering Physical Model of Steam Condensation and the Experimental Study on the Initial Droplet Size Distribution. *Int. J. Therm. Sci.* **2009**, *48*, 2228−2236.

(24) Beysens, D. Dew Nucleation and Growth. *C. R. Phys.* **2006**, *7*, 1082−1100.

(25) Loglio, G.; Ficalbi, A.; Cini, R. A New Evaluation of the Surface Tension Temperature Coefficients for Water. *J. Colloid Interface Sci.* **1978**, *64*, 198.

(26) Miljkovic, N.; Enright, R.; Wang, E. N. Modeling and Optimization of Superhydrophobic Condensation. *J. Heat Transfer* **2013**, *135*, 111004.

(27) Luo, Y.; Li, J.; Zhu, J.; Zhao, Y.; Gao, X. Fabrication of Condensate Microdrop Self-Propelling Porous Films of Cerium Oxide Nanoparticles on Copper Surfaces. *Angew. Chem., Int. Ed.* **2015**, *54*, 4876−4879.

(28) Xu, Q.; Li, J.; Tian, J.; Zhu, J.; Gao, X. Energy-Effective Frost-Free Coatings Based on Superhydrophobic Aligned Nanocones. *ACS Appl. Mater. Interfaces* **2014**, *6*, 8976−8980.